*Optica Applicata, Vol. XLIV, No. 2, 2014*
DOI: 10.5277/oa140212

# Simulation of optical spectra of novel $Tl_4CdI_6$ and $Tl_4HgI_6$ optoelectronic crystals

V. Franiv[1*], O. Bovgyra[2], O. Kushnir[1], A. Franiv[2], K.J. Plucinski[3]

[1]Ivan Franko National University of Lviv, Faculty of Electronics,
8, Kyrylo and Mefodii St., Lviv 79005, Ukraine

[2]Ivan Franko National University of Lviv, Faculty of Physics,
8, Kyrylo and Mefodii St., Lviv 79005, Ukraine

[3]Military University of Technology, Electronic Department,
Kaliskiego 2, Warsaw, Poland

[*]Corresponding author: vafraniv@yahoo.co.uk

The results of calculations using local density approximation and generalized gradient approximation: the total energy depending on the volume of the unit cell, the distribution of the total density of states and the partial contributions of electronic orbitals in the band structure of $Tl_4CdI_6$ and $Tl_4HgI_6$ crystals are shown in this paper. The spectra of the real part of the dielectric permittivity, the spectra of the imaginary part of permittivity, the reflection spectra and the absorption coefficient of both crystals are obtained using the Kramers–Kronig method. A comparative analysis of theoretical calculations with experimental data is carried out. Substantial influence of electron–phonon broadening is shown.

Keywords: density functional theory, band structure, density of states, optical properties.

## 1. Introduction

The actual task of microelectronics is the problem of finding new materials to create temperature sensors on their basis. Usually the basic requirements for these materials are: optimal size, maximum transformation ratio of signal, available temperature range operation, recurrent use of the material in service. Promising in this regard may be crystals that exhibit structural phase transitions of the anomalous behavior of the thermal expansion coefficient. Among the existing compounds, a considerable attention attracted $A_4BX_6$ crystals. Thus, $Tl_4CdI_6$ and $Tl_4HgI_6$ represent a relatively new class of superionics that can exhibit high-temperature phase transitions. Moreover, these new materials with controlled physical parameters are promising compounds for optoelec-

tronics and nonlinear optics. Earlier studies [1–4] described methods of synthesizing these compounds, methods of growth, as well as some results of their physical properties. In this paper we presented the results of calculations of the energy band spectrum and optical constants of $Tl_4CdI_6$ and $Tl_4HgI_6$ crystals. Until now we have not found in literature any work either experimental or theoretical on the optical functions or first principles electronic structure of single-crystalline ternary halides like $Tl_4CdI_6$ and $Tl_4HgI_6$.

## 2. Calculation technique

The calculations of the total electron energy of crystals were carried out self-consistently in the density functional theory framework. The electron energies and densities were determined by solving the Kohn–Sham equations [5]. The method of generalized gradient approximation (GGA) was used to describe the exchange-correlation potential. In this work, we used the Perdew–Burke–Ernzerhof (PBE) representation [6] for this potential. Vanderbilt ultrasoft pseudopotentials [7] were used for the description of ionic potentials. The inequality $\Delta E < 2\times10^{-6}$ eV for the electron energy difference between consequent iterations was selected as a criterion of self-consistent procedure convergence.

The relaxation procedure was considered to converge when the magnitudes of forces acting upon the atoms became less than 0.05 eV/Å and the bulk stress was less than 0.1 GPa. The equilibrium volume $V_0$ (the unit cell volume, at which the total energy is minimal), the bulk modulus of compression $B_0$, and its derivative were obtained from the equation of state of the third order [8, 9], which was fitted to the total energy dependence on the unit cell volume using the least square method.

## 3. Results and discussion

### 3.1. Total energy and structural properties of $Tl_4CdI_6$

In order to check how the experimental lattice parameters differ from the equilibrium one, the geometry optimization of a model structure was carried out.

The experimental and theoretical values for equilibrium lattice parameters and ion positions in the crystal unit cell, as well as the ground state parameters $E_0$, $V_0$, $B_0$, and $B'$, are tabulated. The calculated values of crystal lattice parameters differ from experimental ones within 5.15%, whereas the ion positions differ from the corresponding experimental data by no more than 1.5%.

On the basis of equilibrium structural lattice parameters we obtained the band-energy spectrum of $Tl_4CdI_6$ crystals (Fig. 1).

The analysis of band diagrams showed that those bands which form a forbidden gap demonstrate a rather weak dispersion. There should be noted the greater dispersion in the valence band diagram for the case of equilibrium lattice parameters, and small

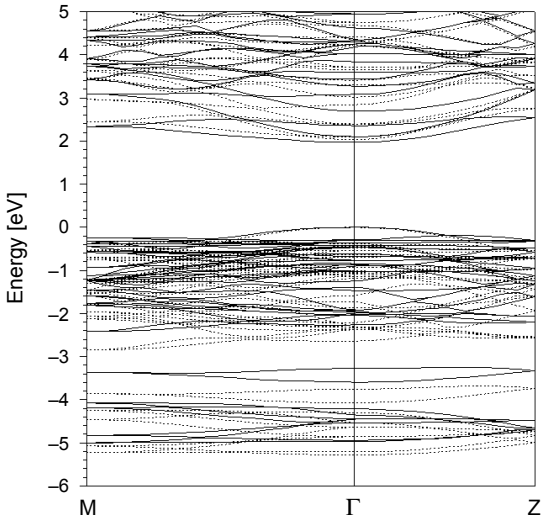


Fig. 1. Fragments of the band-energy diagram for the experimental $Tl_4CdI_6$ crystal lattice constants (dashed line) and theoretical equilibrium structural parameters (solid lines).

decrease in the band gap (0.2 eV). Distribution of states remains unchanged, the width of valence zones complex increases.

### 3.2. Band structure of $Tl_4CdI_6$

First principle calculations of electronic band dispersion of $Tl_4CdI_6$ single crystals are carried out using the Vanderbilt ultrasoft pseudopotential to describe the electron–ion interaction and various approximations of the electrons exchange-correlation interaction, namely: the local density approximation (LDA), generalized gradient approximation (GGA) [6] and hybrid functional B3LYP [10–12].

The calculations were performed with the basis of plane waves (the cut-off kinetic energy $E_{cut}$ = 290 eV).

Figure 2 shows fragments of band-energy diagram $Tl_4CdI_6$ crystal, calculated using the exchange-correlation potentials LDA and GGA. Results of examination show that the zones which form the forbidden gap exhibit rather weak dispersion except towards the center of the Brillouin zone. The smallest band gap energy is located in the center of the Brillouin zone (point $\Gamma$). The band gap in the case of calculations using the LDA approximation is $E_g$ = 1.88 eV (previous calculations show the value 1.78 eV [11]), whereas in the case of GGA – $E_g$ = 2.04 eV.

The analysis of the partial contributions of individual orbitals to the total density of states function and the partial contributions of zones in electron density allowed us to determine the origin of the valence bands of $Tl_4CdI_6$ crystals. The lowest zones are located near –12 eV, showing the localization of the charge on the anion ions (iodine).

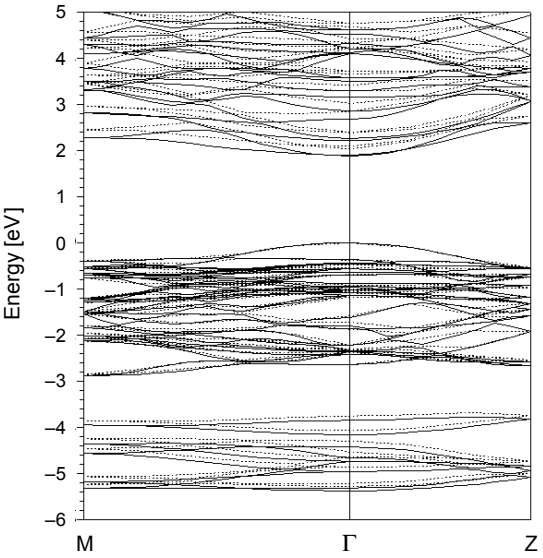


Fig. 2. Fragments of the band-energy diagram for the $Tl_4CdI_6$ crystal calculated using the exchange-correlation potential LDA (solid lines) and GGA (dashed lines).

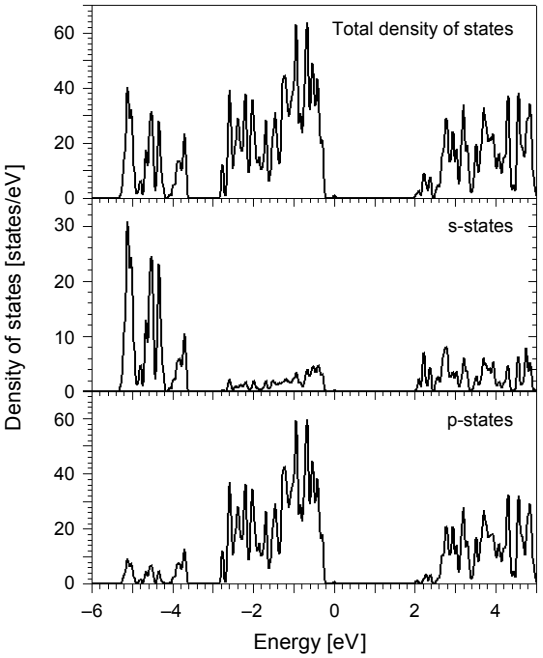


Fig. 3. The distribution of total density of states and the partial contributions of electron orbitals in the band structure of the $Tl_4CdI_6$ crystal.

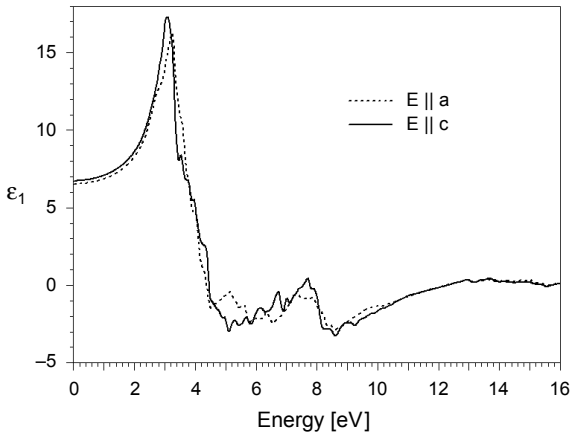


Fig. 4. The real part of dielectric permittivity $\varepsilon_1$ obtained on the basis of band calculations.

The review of contributions of band states by changing the *k*-points involved in the creation of these zones shows only unbound 5*s*-electrons of halogen, as evidenced by the core nature of these zones dispersion. Following Fig. 2, one can emphasize that main mobile holes are near the $\Gamma$ Brillouin zone point. However, more interesting is a fact that along the $\Gamma$–*M* direction there is a coexistence of high and low mobility carriers which may be a confirmation of the coexistence of different bands (see Figs. 3 and 4).

The next valence bands placed around –10 eV are formed by thallium 5*d*-states, whereas Cd 4*d*-states form zones around –8 eV energy mark. Formation of energy bands in the vicinity of labels from –5.5 to –3.5 eV is derived from the contributions of all ions. The nature of these zones is due to intramolecular binding interaction. In all *k*-space these zones are associated with *s*-electron states of thallium and cadmium which overlap with *p*-electron states of iodine.

The next zones in the range from –2.8 to –0.2 eV are associated with the *p*-orbitals of iodine. The top of valence complex is practically anionic with admixture of *s*-states of thallium. States of the bottom of the conduction band are mainly composed of *s*-orbitals of cadmium mixing with thallium *p*-orbitals. Comparing the theoretical results with experimental data we need to remember the underestimation of the value of the band gap in the GGA calculations.

### 3.3. Optical constants dispersion of $Tl_4CdI_6$

Among the optical constants, a particular importance has the real $\varepsilon_1$ and imaginary $\varepsilon_2$ parts of the dielectric constant. This is due to the fact that their spectra, as well as reflectivity spectra can be obtained in a wider energy range compared to other optical functions such as the refractive index *n* and absorption coefficient $\kappa$.

However, the experimental reflectivity curve and the set of optical constants, calculated on their basis, give the integral curve as the sum of contributions of all transitions throughout the volume of the Brillouin zone.

Spectra of the imaginary part of the dielectric function can be obtained from the results of band calculations of wave functions and energy eigenvalues of valence and virtual states. In the imaginary part two types of electronic excitations have contributions: intra- and inter-band ones.

### 3.4. Band structure of $Tl_4HgI_6$

The first principle calculations of electronic band dispersion of $Tl_4HgI_6$ single crystals are carried out using the Vanderbilt ultrasoft pseudopotential to describe the electron –ion interaction and various approximations to describe the exchange–correlation interaction of electrons [6] and hybrid functional B3LYP [10, 11, 13].

The calculations were performed with the basis of plane waves (the cut-off kinetic energy $E_{cut} = 350$ eV). The smallest band gap energy is located in the center of the Brillouin zone (point $\Gamma$). The band gap in the case of calculations using the LDA approximation is $E_g = 1.15$ eV (previous calculations show the value 1.27 eV [11]), whereas in the case of GGA – $E_g = 1.265$ eV. Similar calculations using the hybrid potential B3LYP give the value $E_g = 2.795$ eV. Thus, the $Tl_4HgI_6$ crystals have a direct energy gap.

The analysis of the partial contributions of individual orbitals to the total density of states function (Fig. 3) and the partial contributions of zones in electron density allowed us to determine the genesis of the valence bands of $Tl_4HgI_6$ crystals. The lowest zones located near –12.5 eV show the localization of the charge on the anion ions (iodine). The review of contributions of band states by changing the *k*-points involved in the creation of these zones shows only unbound 5*s*-electrons of halogen, as evidenced by the core nature of these zones dispersion.

### 3.5. Optical constants of $Tl_4HgI_6$

To investigate the optical properties of $Tl_4HgI_6$ crystals, the imaginary part of dielectric permittivity (Fig. 6) has been calculated. On its basis, using the Kramers–Kronig relations [14], the spectral dependences of the reflectance (Fig. 7) and absorption (Fig. 8) have been calculated.

The spectral dependences of $\varepsilon_1$ and $\varepsilon_2$, calculated on the basis of the energy band results, show anisotropy, which is confirmed by comparing the experimental data for two polarizations of light: $E \parallel a$ and $E \parallel c$.

The dependences of optical constants of $Tl_4HgI_6$ crystals can be divided into three main groups of peaks localized in spectral regions: 2–3.5 eV, 3.5–7 eV, and 8–13 eV.

The energy difference between the two curves for different polarizations of light matches the energy distances between the structures that form the bottom of the con-

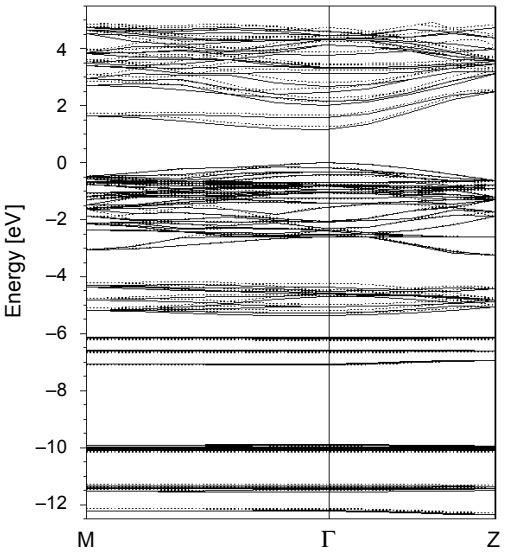


Fig. 5. Fragments of the band-energy diagram for the $Tl_4HgI_6$ crystal calculated using the exchange–correlation potential LDA (solid lines) and GGA (dashed lines).

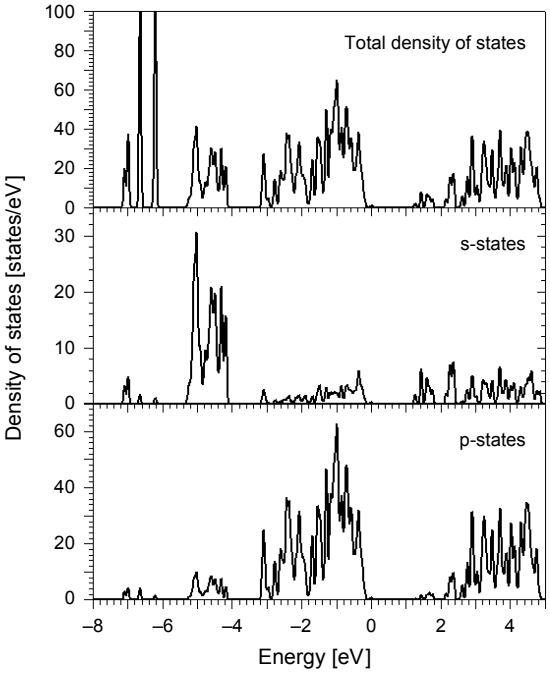


Fig. 6. The total density of states and the partial contributions of electronic orbitals in the band structure of the $Tl_4HgI_6$ crystal.

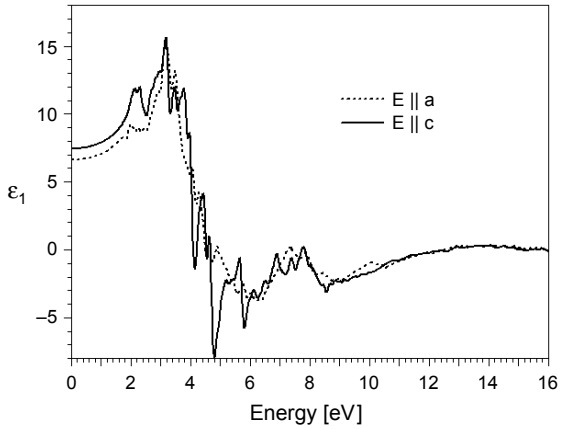


Fig. 7. The real part of dielectric permittivity $\varepsilon_1$ obtained on the basis of band calculations.

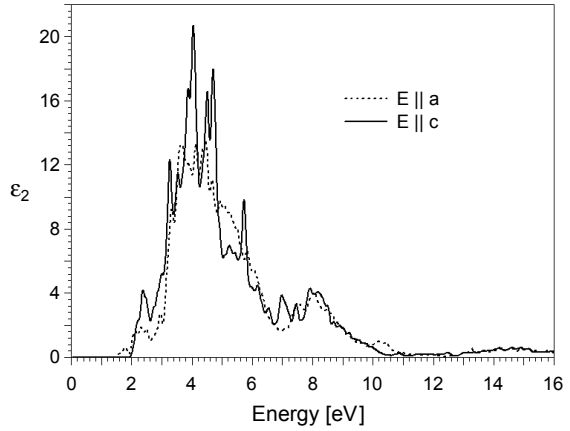


Fig. 8. The imaginary part of dielectric permittivity $\varepsilon_2$ obtained on the basis of band calculations.

duction band of $Tl_4HgI_6$ crystals (compare Figs. 5–8). This is also consistent with experimental data band gap difference for different polarizations obtained from the measured absorption spectra [3].

The performed results show that electron–phonon interaction gives principal contribution to the optical spectra which may define principal features of different materials [14–21].

From the performed calculations of optical functions we have defined the degree of electron–phonon interaction for the principal bands following the technique of Green function calculations [22]. All the spectrum on that basis could be divided into three principal parts. The first one within the 4.1–6.2 eV shows contribution of about 21%, the second one within 6.2–7 eV shows contribution of about 8% and the last one above 7.2 eV – the contribution of 3%.

The obtained results may be useful for further studies of the transparent windows in the IR spectra range. Additionally, they will give information about the mobility of principal carriers, which is crucial for IR optoelectronics.

## 4. Conclusions

For the first time, the band structure calculations using local density approximation and generalized gradient approximation of band-energy diagram, the total energy dispersion depending on the volume of the unit cell were performed. The dispersion of optical functions indicates the substantial contribution of the phonon subsystem. All the spectrum can be divided into three principal parts (4.1–6.2 eV, 6.2–7 eV and above 7.2 eV). The distribution of the total density of states and the partial contributions of electronic orbitals in the band structure of $Tl_4CdI_6$ and $Tl_4HgI_6$ crystals are explored. The spectra of the real part of the dielectric permittivity, the spectra of the imaginary part of permittivity, the reflection spectra and the absorption coefficient of both crystals are obtained using the Kramers–Kronig method.

### References

[1] Badikov D.V., Badikov V.V., Kuz'micheva G.M., Panyutin V.L., Rybakov V.B., Chizhikov V.I., Shevyrdyaeva G.S., Shcherbakova E.S., *Growth and X-ray diffraction study of $Tl_4HgI_6$ crystals*, Inorganic Materials **40**(3), 2004, pp. 314–320.

[2] Piasecki M., Lakshminarayana G., Fedorchuk A.O., Kushnir O.S., Franiv V.A., Franiv A.V., Myronchuk G., Plucinski K.J., *Temperature operated infrared nonlinear optical materials based on $Tl_4HgI_6$*, Journal of Materials Science: Materials in Electronics **24**(4), 2013, pp. 1187–1193.

[3] Franiv A.V., Kushnir O.S., Girnyk I.S., Franiv V.A., Kityk I., Piasecki M., Plucinski K.J., *Growth, crystal structure, thermal properties and optical anisotropy of $Tl_4CdI_6$ single crystals*, Ukrainian Journal of Physical Optics **14**(1), 2013, pp. 6–14.

[4] Hohenberg P., Kohn W., *Inhomogeneous electron gas*, Physical Review **136**(3B), 1964, pp. B864–B871; Kohn W., Sham L.J., *Self-consistent equations including exchange and correlation effects*, Physical Review A **140**(4), 1965, pp. A1133–A1138.

[5] Perdew J.P., Burke K., Ernzerhof M., *Generalized gradient approximation made simple*, Physical Review Letters **77**(18), 1996, pp. 3865–3868

[6] Vanderbilt D., *Soft self-consistent pseudopotentials in a generalized eigenvalue formalism*, Physical Review B **41**(11), 1990, pp. 7892–7895.

[7] Birch F., *Finite strain isotherm and velocities for single-crystal and polycrystalline NaCl at high pressures and 300 K*, Journal of Geophysical Research: Solid Earth **83**(B3), 1978, pp. 1257–1268.

[8] Cohen R.E., Gülseren O., Hemley R.J., *Accuracy of equation-of-state formulations*, American Mineralogist **85**(2), 2000, pp. 338–344.

[9] Becke A.D., *Density functional thermochemistry. III. The role of exact exchange*, The Journal of Physical Chemistry **98**(7), 1993, pp. 5648–5652.

[10] Klintenberg M., Derenzo S.E., Weber M.J., *Potential scintillators identified by electronic structure calculations*, Nuclear Instruments and Methods in Physics Research Section A: Accelerators, Spectrometers, Detectors and Associated Equipment **486**(1–2), 2002, pp. 298–302.

[11] Adamiv V.T., Burak Ya.V., Kityk I.V., Kasperczyk J., Smok R., Czerwiński M., *Nonlinear optical properties of $Li_2B_4O_7$ single crystals doped with potassium and silver*, Optical Materials **8**(3), 1997, pp. 207–213.

[12] STEPHENS P.J., DEVLIN F.J., CHABALOWSKI C.F., FRISCH M.J., *Ab initio calculation of vibrational absorption and circular dichroism spectra using density functional force fields*, The Journal of Physical Chemistry **98**(45), 1994, pp. 11623–11627.

[13] CHENGTEH LEE, WEITAO YANG, PARR R.G., *Development of the Colle–Salvetti correlation-energy formula into a functional of the electron density*, Physical Review B **37**(2), 1988, pp. 785–789.

[14] SHPOTYUK O.I., KASPERCZYK J., KITYK I.V., *Mechanism of reversible photoinduced optical effects in amorphous $As_2S_3$*, Journal of Non-Crystalline Solids **215**(2–3), 1997, pp. 218–225.

[15] RYBAK O., BLONSKII I.V., BILYI YA.M., LUN YU., MAKOWSKA-JANUSIK M., KASPERCZYK J., BERDOWSKI J., KITYK I.V., SAHRAOUI B., *Luminescent Spectra of $PbI_2$ single crystals doped by 3d-metal impurities*, Journal of Luminescence **79**(4), 1998, pp. 257–267.

[16] WASYLAK J., KUCHARSKI J., KITYK I.V., SAHRAOUI B., *Photoinduced effects in the $Sb_2Se_3$-$BaCl_2$-$PbCl_2$ glasses*, Journ of Applied Physics **85**(1), 1999, pp. 425–431.

[17] KITYK I.V., KASPERCZYK J., PLUCINSKI K., *Two-photon absorption and photoinduced second-harmonic generation in $Sb_2Te_3$-$CaCl_2$-$PbCl_2$ glasses*, Journal of the Optical Society of America B **16**(10), 1999, pp. 1719–1724.

[18] PLUCIŃSKI K.J., GRUHN W., KITYK I.V., IMIOŁEK W., KADDOURI H., BENET S., *Photoinduced second harmonic generation in $Bi_2Se_3$-$CaBr_2$-$PbCl_2$ optical fibers*, Optics Communications **204**(1–6), 2002, pp. 355–361.

[19] GRUHN W., KITYK I.V., EBOTHE J., KARAFIAT A., KOZARZEWSKI B., BENET S., *Appearance of ferroelectricity in thin $Se_xTe_{1-x}$ crystalline films*, Materials Science and Engineering B **96**(3), 2002, pp. 263–267.

[20] KITYK I.V., *IR-induced second harmonic generation in $Sb_2Te_3$-$BaF_2$-$PbCl_2$ glasses*, The Journal of Physical Chemistry B **107**(37), 2003, pp. 10083–10087.

[21] KITYK I.V., *IR-stimulated second harmonic generation in $Sb_2Te_2Se$-$BaF_2$-$PbCl_2$ glasses*, Journal of Modern Optics **51**(8), 2004, pp. 1179–1189.

[22] ANTONYAK O.T., PIDZYRAILO N.S., *Spectroscopy of activator centers of different local symmetry in $SrCl_2$*, Optics and Spectroscopy **69**(3), 1990, pp. 361–364.

*Received August 6, 2013*
*in revised form September 11, 2013*